THREE-DIMENSIONAL SIMULATION OF PSEUDO-DUCTILE BEHAVIOR OF ANGLE-PLY AND CROSS ANGLE-PLY LAMINATES

Xi Deng*[1], Wen-Xue Wang[2], T. Matsubara[2]
[1] Department of Aeronautics and Astronautics, Engineering School, Kyushu University, Motooka Nishi-ku Fukuoka 819-0395, Japan
(* E-mail: dengxi147@outlook.com)
[2] Research Institute for Applied Mechanics, Kyushu University, Kasuga, Fukuoka 816-8580, Japan

Keywords: Microscopic model, Angle-ply laminate, Cross angle-ply laminate, Pseudo-ductility

ABSTRACT

Carbon fiber reinforced polymer (CFRP) composites have occupied more important position for excellent mechanical properties, which are limited by brittle failure under loads meanwhile. For this reason, recent researches are mainly focused on improving non-linear behaviour of CFRP. This non-linear behaviour can be thought as a pseudo-ductile response. This paper proposes a three-dimensional (3-D) mesoscale model for the finite element analysis of nonlinear stress–strain responses of CFRP angle-ply $[\pm\theta]_{2s}$ and cross angle-ply $([\theta/-\theta/(90+\theta)/(90-\theta)]_s$ laminates. One ply of the laminate model contains three fiber layers. Fiber orientation θ varies from 15º to 45º for angle-ply laminates and varies from from 10º to 35º for cross angle-ply laminates, respectively. Predictions of the nonlinear stress-strain responses of various angle-ply agree well with previous experimental results, which verifies that the present mesoscale model is available for the prediction of the pseudo-ductile behaviour of angle-ply laminates. Cross angle-ply laminates give about 50% lower pseudo-ductile strain than that of angle-ply laminates. Large fiber orientation angle yields high pseudo-ductile strain for both of angle-ply and cross angle-ply laminates.

1. Introduction

Carbon fiber reinforced polymer (CFRP) composites are widely used in many industrial products, such as aircrafts, aeronautic structures, automobiles, transportation vehicles, and wind turbine blades due to the outstanding mechanical properties, such as superior specific strength and specific modulus, thermo-stability, etc. However, their benefits are often limited by their sudden, brittle and catastrophic failure with little or without warning [1]. For the sake of safe operation, much higher safety margins are usually applied to CFRP composites in the design of composite structures than to relatively ductile materials, such as metals. These design limitations reduce the advantages of light weight, high stiffness and high strength of CFRP and preclude the realization of the full potential in many practical applications. For this reason, achieving more non-linear stress–strain response, with the ability to yield and extension as metals, is highly desirable in recent years [2-5]. A parameter, pseudo-ductile strain is newly introduced to describe the non-linear behaviour of composites to distinguish the conventional ductile behaviours of metals from the ductile-like nonlinear stress-strain behaviours of fiber reinforced polymer (FRP) composite materials [3]. Several ways are developed to enhance the non-linear property of CFRP composites.

One way is adding other fiber laminas into CFRP, which yields hybrid fiber reinforced composites. These two sorts of fiber laminas possess high and low failure strain, respectively. Therefore, a proper hybrid of these two fiber laminas can make the hybrid composites bear more stress at a relative high strain, compared to original CFRP. Czél et al. [3] calculated the mode II inter-laminar fracture behaviour of a three layer ply-by-ply glass/carbon hybrid composite laminate and predicted the allowable central carbon layer thickness for stable pull-out. Stable failure to high strains has been successfully demonstrated on thin carbon prepreg reinforced hybrid composites. The crucial role of the central carbon ply in a unidirectional (UD) laminate, through observing the changes of fracture, is mainly affected by the carbon layer thickness. Jalalvand et al. [4] proposed a FEM model to simulate all the possible damage models in $[G/C_n/G]$ (n=1~2) and $[G_2/C_m/G_2]$ (m=1~4) glass/carbon hybrid UD composites in uniaxial tension tests. The proposed method is validated against the experimental results

and then used to simulate the progressive damage process of other hybrid configurations. As a result, a damage-mode map was produced for this material set, with which the method can easily be applied to other hybrid composites to assess their performance.

The second way is changing the design of the fiber orientation and stacking order of laminates [6, 7], which can improve the non-linear property of the composites as well. Fuller et al. [6] used a thin angle-ply carbon–epoxy prepreg material with a cured ply thickness of 0.03 mm, which is developed via High Performance Ductile Composite Technology program (HiPerDuCT) [8, 13, 14], and gained a highly non-linear behavior of stress–strain response. The pseudo-ductility of the angle-ply laminate of thin ply CFRP increases with the increase of the fiber angle from 15° to 45°. Laminates $[\pm 25]_{5s}$ and $[\pm 30]_{5s}$ show failure strains of 3.6% and 5.4% (an increase by a factor of 1.5), and the pseudo-ductile strains of 1.2% and 2.88%, respectively, whilst the tensile strength reduces by only 25% for $[\pm 30]_{5s}$. Based on the X-ray computed tomography and microscopy, it is proved that fiber rotation and matrix plasticity considerably affect the failure strain and the pseudo-ductile strain. However, existing studies involved the development of pseudo-ductility of CFRP composites are limited to one direction pseudo-ductility composite materials or UD composite materials.

In the present work, more than one directional ductility, that is, pseudo-ductility in two perpendicular directions of CFRP laminates is taken into account. A new type of CFRP laminates $[\theta/-\theta/(90+\theta)/(90-\theta)]_s$ is proposed based on idea of the combination of angle-ply laminate and cross-ply laminate and is named cross angle-ply laminates. This type of laminates has two mutually perpendicular angle-ply layers and is expected to have identical non-linear material property in the two perpendicular directions of the laminates and have better failure tolerance. Numerical simulations for the cross angle-ply laminates subjected to tensile loading are carried out using a finite element analysis (FEA) code of MSC MARC 2011. The nonlinear and pseudo-ductile responses of the cross angle-ply laminates are predicted for various angle θ. For the comparison and validation of numerical analysis results, numerical simulations of angle-ply laminates $[\pm\theta]_{2s}$ subjected to tension are also conducted. The predicted nonlinear stress-strain curves of angle-ply laminates $[\pm\theta]_{4s}$ for various angle θ are compared to the previous experimental results [6]. The effect of angle θ on the nonlinear stress-strain behavior of the cross angle-ply laminates $[\theta/-\theta/(90+\theta)/(90-\theta)]_s$ is investigated.

2. Numerical analysis

2.1 Microscale model and material constants

A three-dimensional and full thickness microscale model is developed in this paper, which is different from previous two-dimensional models [7-9] based upon classical laminate analysis theory, from the homogeneous and orthotropic elastoplastic models [10-12, 17]. One ply contains three layers of fibers and the thickness of one ply is 0.03 mm. Figure 1 shows partial region of one ply with fiber

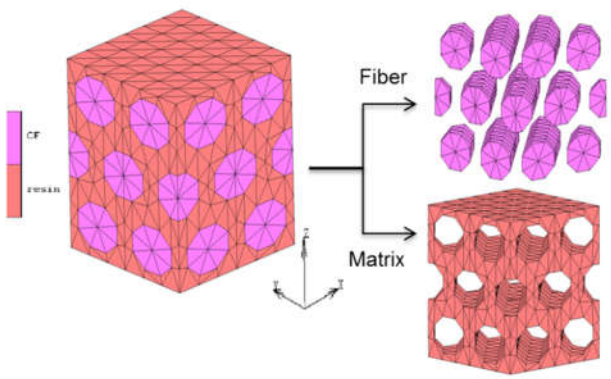

Figure 1: Partial region of one ply with fiber angle 45° in the microscale model.

angle 45° in the microscale model. An ideal uniform distribution of fibers is assumed for the first research step and the fiber is approximated by a regular octagonal prism for the simplicity of mesh of

the model. The pink parts represent fibers and orange parts represent matrix resin. The carbon fiber volume fraction of the model is 0.42 for the convenience of comparison with previous experimental [6]. There is no interface element inserted between the fiber and matrix in the present analysis due to the limitation of computational ability of our personal computer. The fiber is considered as linearly elastic and transversely isotropic and the matrix resin is assumed as elastoplastic. The material constants of fiber and resin are listed in Table 1, in which shear modulus G_{23} for fiber is calculated using transversely isotropic material theory.

Constants	Carbon fiber	Resin
E_1(MPa)	234000	3300
E_2=E_3(MPa)	13000	
μ_{12}= μ_{13}	0.2	0.38
μ_{23}	0.3	
G_{12}=G_{13}(MPa)	15000	1200
G_{23}(MPa)	5000	

Table 1 Material constants of carbon fiber and resin

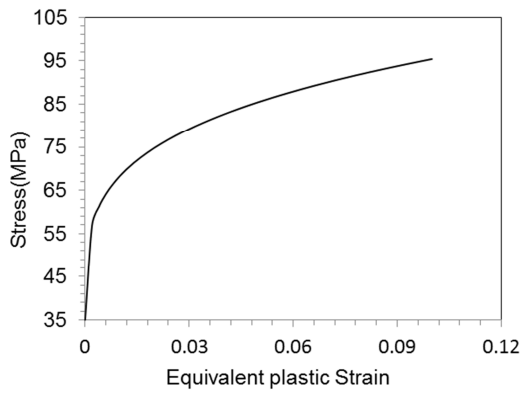

Figure 2: Stress-equivalent plastic strain curve of matrix resin.

In order to describe the nonlinear stress-strain behavior of angle-ply and cross angle-ply laminates, suitable description of elastoplastic behavior of resin is quite important because the stress-strain response of resin in the microscale region in the composite is different from that in block material scale of resin [6]. In present study, the relationship of stress and effective plastic strain is expressed by following equation.

$$\sigma_m = A\left(\varepsilon_m^p\right)^r + \sigma_y \tag{1}$$

Where A is a constants, σ_m means matrix stress, σ_y means initial yield stress and ε_m^p means matrix effective plastic strain. It is seen that the effective plastic strain is expressed by a power law term. According to the curve fitting in previous studies [6, 7], A=9.2×10^{-32}, r=3.86, σ_y=35MPa are used in present analysis. The stress- equivalent plastic strain curve of resin is described in Fig. 2.

To predict the failure of laminates, maximum strain criteria are applied for the failure prediction of both carbon fiber and resin, respectively. Referring to previous data [6, 7], failure parameters listed in Table 2 are used in the present analysis. In addition, progressive failure of the laminate is adopted with residual stiffness factor of 0.01. That is, as soon as the strain in an element arrives at its critical value the element the stiffness value is reduced to the 0.01 of its initial stiffness.

Microscale models of through thickness for angle-ply laminates $[45/-45]_{2s}$ and cross angle-ply laminate $[30/-30/120/60]_s$ are presented in Fig. 3 and Fig. 4. The cross angle-ply laminate $[\theta/-\theta/90+\theta/90-\theta]_s$ is newly proposed laminate in this research to develop laminates with

pseudo-ductility in two orthogonal directions because angle-ply laminates can achieve at excellent pseudo-ductility and acceptable strength in only one direction and has poor mechanical properties in the perpendicular direction. It is expected that the cross angle-ply can provide reasonable pseudo-ductility and acceptable strength in two orthogonal directions. Each microscopic model contains four plies, each ply is 0.03 mm thick and contains three fiber layers. The thickness of both models is 0.12 mm. The x-axis direction is parallel to the loading direction, y-axis direction is along the width direction of the laminate, and z-axis direction is along the thickness direction of the laminate. Only upper half of the laminate is modeled because of the symmetry of the laminates. Symmetrical boundary conditions are applied to the z = 0 plane (the mid-plane of the laminate) and stress free conditions are applied to the top surface of the model. The other four surfaces are subjected to periodic boundary conditions. The details will be described in next subsection.

Maximum strain criterion	Carbon fiber	Resin
Max tensile strain X	0.019	0.08
Max compress strain X	0.013	0.12
Max tensile strain Y/Z	0.08	
Max compress strain Y/Z	0.1	
Max shear strain S_{12},S_{13}	0.35	0.35
Max shear strain S_{23}	0.35	

Table 2 Failure criteria of carbon fiber and resin

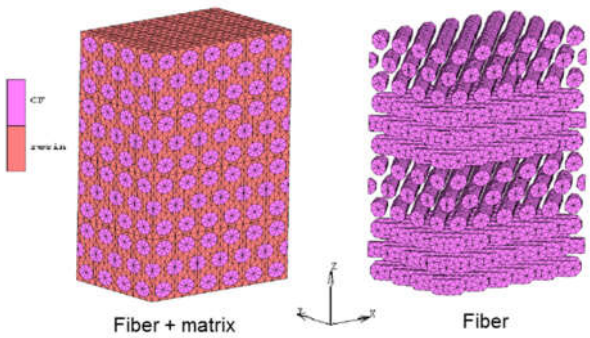

Figure 3: Microscale model for $[45/-45]_{2s}$ angle-ply laminate.

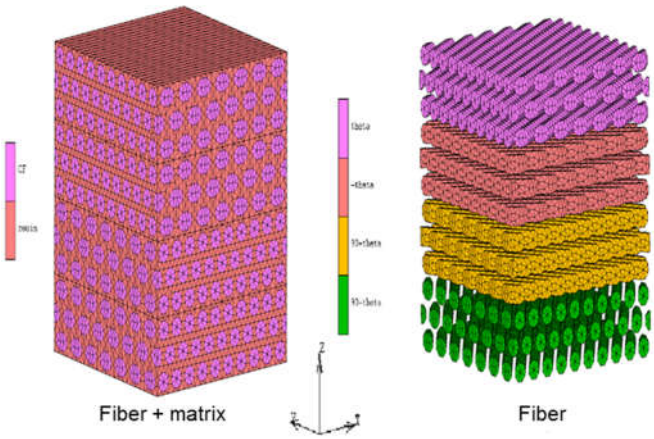

Figure 4: Microscale model for $[35/-35/125/55]_s$ cross angle-ply laminate.

2.2 Meshes and periodic boundary conditions

From Fig. 3 and Fig. 4, it is seen that the microstructures of both models are quite complicate although they are still far from the real composite laminates in which there are much and much more fibers. It is difficult to make the regular meshes for both models. Auto-mesh function of the software of MSC Marc 2011 is utilized to make the meshes of both models based on the pre-made 3-D solid models. According to the instructions related to nonlinear analysis of MSC Marc 2011, high-order 10 nodes isoparametric tetrahedral element (element number 127) is used because of the strong nonlinear behaviors of angle-ply laminates reported in [6, 7]. Besides, cohesive interface element is not used in the present analysis since little delamination occurs in the laminates consisting of present such thin plies [13-17]. The model for angle-ply laminate has 70208 elements and 99707 nodes, and the model for cross angle-ply laminate has 117101 elements and 164362 nodes. It is worth noting that more large models containing more fibers and having the same width and gauge length as the standard CFRP tensile specimen are desirable to simulate the tensile testing of these laminates. However, it is almost impossible to make such large microscale models because of the limitation of computational ability of our personal computers. Thus, a periodic repeatable representative model is necessary to reduce the computational cost. As seen in Fig. 3 and Fig. 4, the width and length of the present models are less than the thickness due to the limitation of computational ability of our personal computers. Therefore, proper periodic boundary conditions must be applied to the surfaces of x = 0 and x = a, and surfaces of y = 0 and y = b to ensure the compatibility of the displacement fields on the opposite faces of the model, as expressed follows.

$$u_i^+(a,y,z) - u_i^-(0,y,z) = \delta_{yz-i} \qquad (i = x,y,z) \tag{2}$$

$$u_i^+(x,b,z) - u_i^-(x,0,z) = \delta_{xz-i} \qquad (i = x,y,z) \tag{3}$$

Where u_i^+ and u_i^- are the nodal displacements on the opposite pair surfaces of the model, δ_{yz-i} and δ_{xz-i} are unknown constants, a and b are the length in x-direction and width in y-direction of the model, respectively. These periodic boundary conditions imply that both of the opposite pair surfaces of the models must have parallel deformation, as depicted in Figure. 5.

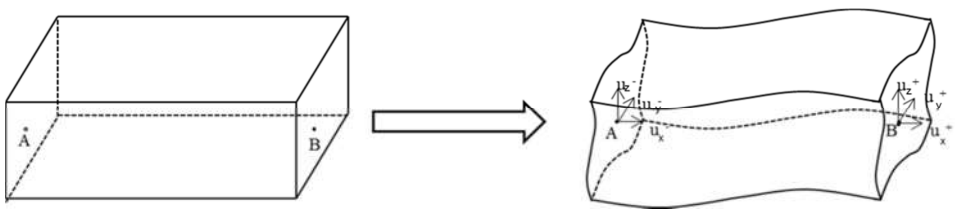

Figure 5: Periodic boundary conditions for a representative model.

In order to easily apply the periodic boundary conditions to the opposite pair surfaces of the model, congruent meshes on the pair surfaces are desirable. In other words, it should be better that the pair surfaces have the same mesh configuration and same in-surface node coordinates. In the case of angle-ply laminate, it is not difficult to make the congruent meshes for opposite pair surfaces of x = 0 and x = a, and pair surfaces of y = 0 and y = b. On the other hand, it is hard to make the exact congruent meshes for opposite pair surfaces in the case of cross angle-ply laminate since there are four plies with different fiber orientation, and there are errors between the theoretically calculated and actually used digital values of node coordinates. A little modification is adopted to the model to ensure the congruent meshes for opposite pair surfaces in the case of cross angle-ply model. As a result, the fiber orientation θ in the modified model may have slight deviation (less than 0.3°) from originally designed angle. Once the congruent meshes are made for the opposite pair surfaces of the model, the periodic boundary conditions can be applied using the option of "servo-links" in MSC Marc 2011 [18, 19]. Servo-links allow prescribing multi-points nodal displacements as a linear function with constant coefficients, as expressed by Equation. (2) and (3). δ_{yz-i} and δ_{xz-i} are prescribed by creating two new unconstrained nodes, and linking the nodes on the corresponding opposite faces to these two nodes, respectively, which is depicted in Figure 6 (left picture). A symmetrical boundary condition

$u_z(x, y, 0) = 0$ is applied to the bottom (mid-plane of the laminate) of the model, a fixed displacement $u_x(0, y, 0) = 0$ is applied to the left surface of the model, and fixed displacements $u_y(0,0,z) = 0$ and $u_y(a, 0, z) = 0$ are applied to the middle nodes on the left and right surfaces to prevent rigid movement. Uniform tensile displacement is applied to the right surface of the model by applying a displacement to the right unconstrained node.

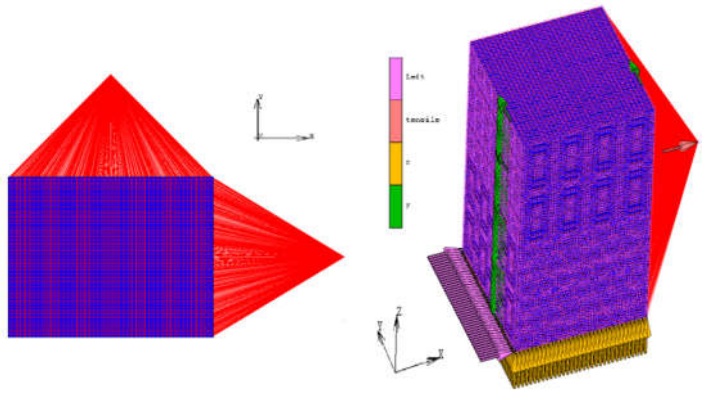

(a) Servo-links (b) Boundary conditions

Figure 6: Servo-links to apply the periodic boundary conditions to the representative model.

2.3 Definition of pseudo ductility

Pseudo-ductility of laminates is affected by fiber fracture in different layers, fiber reorientation variation, and plastic deformation of matrix. Here the word "pseudo" means that the ductility has been achieved through damage development in the composite rather than the ductile behavior which occurs in metals due to sliding of layers of atoms relative to each other at dislocations. This pseudo-ductility of laminates has been proved by loading-unloading-loading test presented in [14, 15]. It can be characterized by pseudo ductile strain, ε_d, which is defined by the difference between the failure strain and the strain at the same stress level on a straight line of initial modulus, as described in Figure 7.

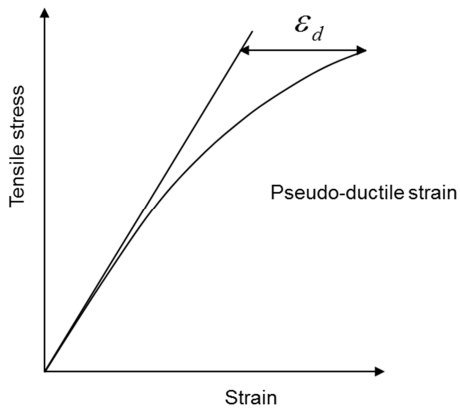

Figure 7: Diagrammatic defination of pseudo-ductile strain

3. Numerical results

3.1 Angle-ply laminates

Simulation results of nonlinear stress-strain curves of $[(\pm\theta)_2]_s$ angle-ply laminates loaded under quasi-static tension are presented in Figure 8, together with previous experimental results of $[(\pm\theta)_5]_s$ angle-ply layups [6]. It is worth noting that it is difficult to construct a full microscopic model for $[(\pm\theta)_5]_s$ angle-ply laminates due to the limitation of computational ability of our personal computer.

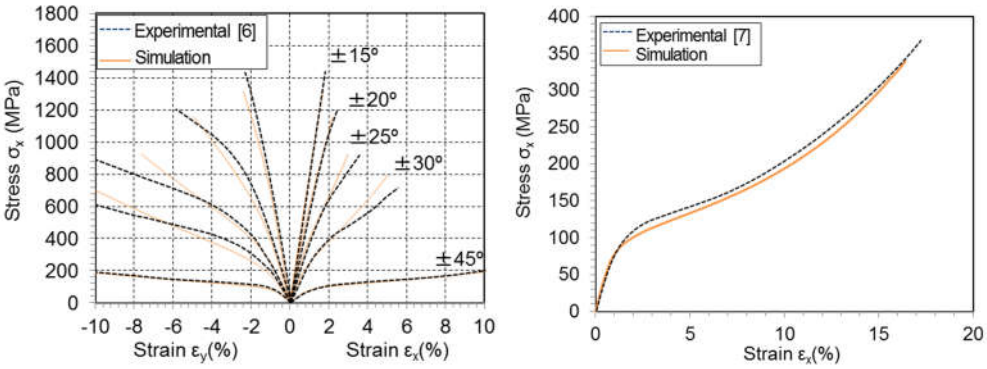

(a) (b)

Figure 8: Stress-strain curves of various angle-ply laminates

Layups	Failure stress (MPa)	Failure strain (%)	Pseudo-ductile strain (%)
$[(\pm 15^{o})_2]_s$	1313	1.70	0.12
$[(\pm 20^{o})_2]_s$	1157	2.20	0.41
$[(\pm 25^{o})_2]_s$	925	3.03	1.07
$[(\pm 30^{o})_2]_s$	785	5.04	2.24
$[(\pm 45^{o})_2]_s$	338	16.88	13.22

Table 3 Failure stress, failure strain and pseudo ductile strain of angle-ply laminates

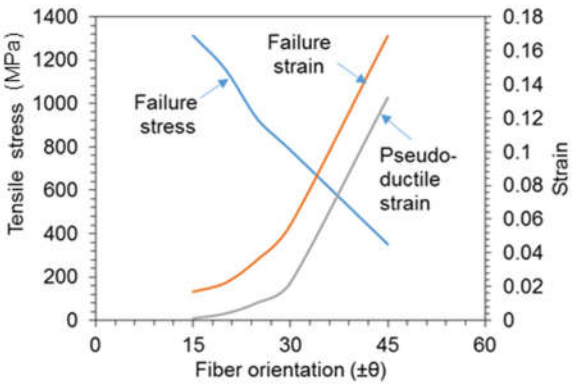

Figure 9: Trade-off relationship between failure stress and pseudo-ductile strain

Instead of the full $[(\pm\theta)_5]_s$ laminates, $[(\pm\theta)_2]_s$ laminates are simulated using a representative model. As displayed in Figure 8, $[(\pm 15^{o})_2]_s$ laminate exhibits a nearly linear response. For the laminates of $\theta > 15°$, all stress-strain curves display three different response regions: an initial linear region, followed by a deviation from the linear region and finally a stiffening region. Fiber breakage dominates the laminate failure due to the fiber arriving at its tensile strength in the laminates of $\theta < 30°$ and matrix failure dominates the laminate failure in the laminates of $\theta \geq 30°$. From Figure 8, it is seen that present simulation curves agree well with the previous experimental results within certain strain range. However, in the cases of very large strain, there are still relatively large difference in both results of present simulation and previous experiment. There are two reasons which may cause the difference. One is the different in the simulation model laminates and the laminated tested in [6].

Another one is that the simulation model is only a representative model, not a full tensile specimen model. It cannot exactly simulate the damage progression from the specimen edge as usually observed during the tensile testing at large tensile strain level. Detail values of tensile failure stress, failure strain, and pseudo-ductile strain are listed in Table 3. Failure stress decreases, failure strain and pseudo-ductile strain increase as the fiber angle increases. Laminates of $[(\pm 15^o)_2]_s$ and $[(\pm 20^o)_2]_s$ show very little pseudo-ductile strain, laminates of $[(\pm 25^o)_2]_s$ and $[(\pm 30^o)_2]_s$ show reasonable pseudo-ductile strains and acceptable high failure stresses. In contrast, $[(\pm 45^o)_2]_s$ gives very large pseudo-ductile strain but very low failure stress, as fully described in Figure 8b. The trade-off relationship between failure stress and pseudo-ductile strain is depicted in Figure 9, which may be useful for the design of angle-ply laminates.

3.2 Cross angle-ply laminates

Cross angle-ply laminates are newly proposed laminates in this research to develop laminates with pseudo-ductility in two orthogonal directions. Simulation results of stress-strain curves of $[\theta/-\theta/(90+\theta)/(90-\theta)]_s$ cross angle-ply laminates loaded under quasi-static tension are presented in Figure 10a. Effects of fiber angle on the failure stress, failure strain, and pseudo-ductile strain are described in Figure 10b. Detail values of failure stress, failure strain and pseudo-ductile strain are listed in Table 4.

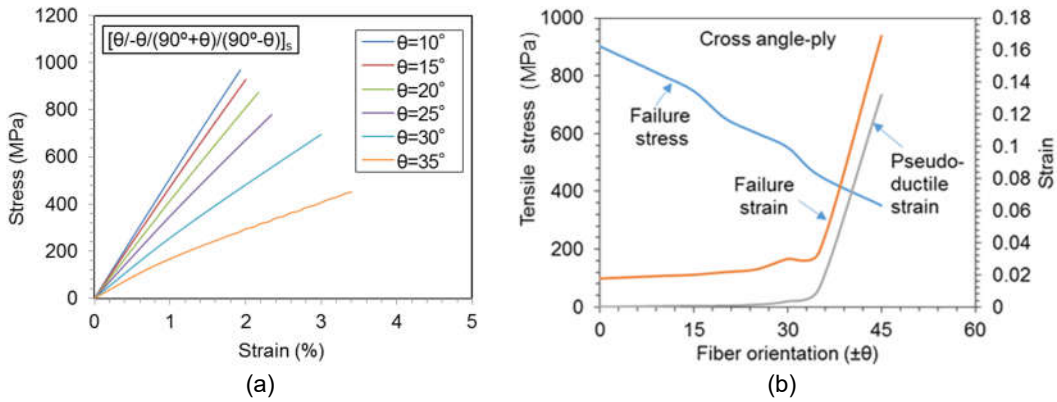

Figure 10: Stress-strain curves of various cross angle-ply laminates

Stacking order	Failure stress (MPa)	Failure strain (%)	Pseudo-ductile strain (%)
$[0^o_2/90^o_2]_s$	902	1.767	0.048
$[10^o/-10^o/100^o/80^o]_s$	801	1.93	0.048
$[15^o/-15^o/105^o/75^o]_s$	747	2.02	0.065
$[20^o/-20^o/110^o/70^o]_s$	653	2.15	0.079
$[25^o/-25^o/115^o/65^o]_s$	602	2.34	0.143
$[30^o/-30^o/120^o/60^o]_s$	552	3.00	0.351
$[35^o/-35^o/125^o/55^o]_s$	455	3.40	1.135

Table 4 Failure stress, failure strain and pseudo ductile strain of cross angle-ply laminates

Similar to the angle-ply laminates, failure stress decreases, failure strain and pseudo-ductile strain increase as the fiber angle increases. For $10° \leq \theta \leq 20°$, the laminate shows a linear stress-strain curve. The fibers in the $\pm\theta$ plies play a main role in bearing the tensile load, while the fibers in the $90° \pm \theta$ plies mainly support transverse load. Hence once the $\pm\theta$ fibers fail, the whole laminate loses its load carrying capacity instantly. For $\theta \geq 20°$, the laminate shows a little linear stress-strain response. The matrix also began to play an important role in holding the fibers together and in bearing the tensile load. The failure strain in two orthogonal directions (x-axis and y-axis) is higher than 2%

for $\theta \geq 15°$, which is the advantage of cross angle-ply laminates compared to ordinary angle-ply laminate. However, the pseudo-ductile strains are many lower than those of relative angle-ply laminates due to the addition of [(90+θ)/(90-θ)] plies. High pseudo-ductile strain can be expected only in the range of $35° < \theta \leq 45°$. Attention should be paid to the trade-off relationship between failure stress and pseudo-ductile strain or failure strain in the design of reasonable cross angle-ply laminates according to practical application.

5. Conclusion

Three-dimensional microscopic models for finite element analysis of angle-ply laminates and cross angle-ply laminates are constructed. A new orthotropic laminate, cross angle-ply laminate $[\theta/-\theta/(90+\theta)/(90-\theta)]_s$ is proposed to make the laminate pseudo-ductile in two orthogonal directions. This laminate consists of two mutually perpendicular angle-ply layers, and is expected to have identical non-linear material property and better failure tolerance in two perpendicular directions of the laminate. Tensile testing of angle-ply laminates and cross angle-ply laminates are simulated using the present microscopic models. Numerical results lead to following conclusions.

Nonlinear stress-strain behaviors of angle-ply laminates and cross angle-ply laminates loaded under quasi-static tension are well simulated using present microscopic models with linear elastic fiber and elastic-plastic matrix. Numerical predictions for angle-ply laminates agree well with previous experimental results, which prove the validity of present microscopic models. Fiber angle has significant effects on failure stress, failure strain and pseudo-ductile strain of laminates. Large pseudo-ductile strain can be obtained from the angle-ply laminates with fiber angle larger than $15°$. Cross angle-ply laminates of $\theta \geq 20°$ show a little linear stress-strain response in two orthogonal directions although the pseudo-ductile strains are many lower than those of relative angle-ply laminates due to the addition of [(90+θ)/(90-θ)] plies. High pseudo-ductile strain is limited to the laminates with $35° < \theta \leq 45°$. Laminate failure is dominated by the fiber breakage for small fiber angle for both angle-ply laminates and cross angle-ply laminates. In the laminates with large fiber angle, matrix failure plays an increasing role in the laminate failure as the fiber angle increases. Experimental research for cross angle-ply is necessary to confirm the validity of the simulation results based on the macroscopic model of cross angle-ply, which is scheduled to conduct tensile testing.

Acknowledgements

The first author would like to express his thanks to the scholarship provided by the China Scholarship Council for study at the Kyushu University

References

[1] M.O.W. Richardson. Review of low-velocity impact properties of composite materials. *Composites Part A: Applied Science and Manufacturing*. 27, 1996, pp. 1123-1131. (doi:10.1016/1359-835X(96) 00074-7)
[2] G. Kretsis. A review of the tensile, compressive, flexural and shear properties of hybrid fiber-reinforced plastics. *Composites*. 18, 1987, pp. 13-23 (doi:10.1016/0010-4361(87)90003-6)
[3] Gergely Czél, M.R. Wisnom. Demonstration of pseudo-ductility in high performance glass/epoxy composites by hybridisation with thin-ply carbon prepreg. *Composites: Part A*. 52, 2013, pp. 23–30 (doi:10.1016/j.compositesa.2013.04.006)
[4] Meisam Jalalvand, Gergely Czél, Michael R. Wisnom. Numerical modelling of the damage modes in UD thin carbon/glass hybrid laminates. *Composites Science and Technology*. 94, 2014, pp. 39–47 (doi:10.1016/j.compscitech.2014.01.013)
[5] HaNa Yu, et al. Pseudo-ductility in intermingled carbon/glass hybrid composites with highly aligned discontinuous fibers. *Composites Part A: Applied Science and Manufacturing*.73, 2015, pp. 35–44 (doi:10.1016/j.compositesa.2015.02.014)
[6] J.D. Fuller, M.R. Wisnom. Pseudo-ductility and damage suppression in thin ply CFRP angle-ply laminates. *COMPOSITES PART A*. 69, 2015, pp. 64-71 (doi:10.1016/j.compositesa.2014.11.004)

[7] J.D. Fuller, M.R. Wisnom. Exploration of the potential for pseudo-ductility in thin ply CFRP angle-ply laminates via an analytical method. *Composites Science and Technology*.112, 2015, pp.8–15 (doi:10.1016/j.compscitech.2015.02.019)
[8] C.T. Sun, J.L. Chen. A Simple Flow Rule for Characterizing Nonlinear Behavior of Fiber Composites. *Journal of Composite Materials*. 23. 1989, pp 1009-1020
[9] C.T. Sun, J.L. Chen. A micromechanical model for plastic behavior of fibrous composites. *Composites Science and Technology*. 40, 1991, pp. 115–129 (doi: 10.1016/0266-3538(91)90092-4)
[10] M. Ridha, T. E. Tay, A. Nettles. Effect of fiber orientations on progressive damage of notched $[\theta/0^{o}/-\theta/90^{o}]_s$ composite laminates. *20th International Conference on Composite Materials,* Copenhagen, 19-24th July 2015.
[11] Alexander Bismarck, Omar Bacarreza, et al. Exploring routes to create high performance pseudo ductile fiber reinforced composites. *20th International Conference on Composite Materials,* Copenhagen, 19-24th July 2015.
[12] P.F. Liu, Z.P. Gu, Y.H. Yang, X.Q. Peng. A nonlocal finite element model for progressive failure analysis of composite laminates. *Composites Part B*. 86, 2016, pp. 178-196 (doi.org/10.1016/j. compositesb.2015.09.061)
[13] Sangwook Sihn, Ran Y. Kim, et al. Experimental studies of thin-ply laminated composites. *Composites Science and Technology.* 67, 2007, pp. 996–1008(doi:10.1016/j.compscitech.2006.06.008)
[14] P. Ladeveze, E. LeDantec. Damage modelling of the elementary ply for laminated composites. *Composites Science and Technology.* 43, 1992, pp. 257–267(doi:10.1016/0266-3538(92)90097-M)
[15] Wisnom M.R, et al. Repeated tensile loading of thin-ply pseudo-ductile laminates. *American Society for Composites 30th Technical Conference on Composite Materials.* Michigan 28-30 Sep 2015
[16] D. Leguillona, G. Marionb, R. Harryb, F. Lécuyerd. The onset of delamination at stress-free edges in angle-ply laminates — analysis of two criteria. *Composites Science and Technology*.61, 2001, pp. 377–382 (doi:10.1016/S0266-3538(00)00105-6)
[17] Tomohiro Yokozeki, Akiko Kuroda, et al. Damage characterization in thin-ply composite laminates under out-of-plane transverse loadings. *Composite Structures*. 93, 2010, pp. 49–57 (doi:10. 1016/j.compstruct.2010.06.016)
[18] MSC Software. MSC Marc 2011 User Documentation. Volume A: theory and user information. Technical report, MSC Software, Santa Ana, CA, USA; 2011
[19] Andrew Drach, Borys Drach, Igor Tsukrov. Processing of fiber architecture data for finite element modeling of 3D woven composites. *Advances in Engineering Software*. 72, 2014, pp 18–27. (doi.org/10.1016/j.advengsoft.2013.06.006)